Available online at www.sciencedirect.com

ScienceDirect

IFAC PapersOnline CONFERENCE PAPER ARCHIVE

IFAC PapersOnLine 56-3 (2023) 61–66

Wind Field Estimation Using Multiple Quadcopters

Hao Chen * **He Bai** * **Clark N. Taylor** **

* *School of Mechanical and Aerospace Engineering, Oklahoma State University, Stillwater, OK 74078 USA (e-mail: {hao.chen,he.bai}@ okstate.edu)*

** *Department of Electrical and Computer Engineering, Air Force Institute of Technology, Wright-Patterson, OH, USA (e-mail: clark.taylor@afit.edu)*

Abstract: We consider a wind field estimation problem with multiple quadcopters. The wind field is assumed to affect the motion of the quadcopters in an additive fashion. Starting with a single quadcopter case, we first design an Extended Kalman filter (EKF) for constant and spatial-varying wind estimation. We next extend the EKF wind estimator for multiple quadcopters with directed connected communication graphs. To fuse the estimates of the wind field, we develop a sequential covariance intersection (SCI) method and a sequential weighted exponential product (SWEP) method for constant and spatially-varying wind fields. The effectiveness of the designed partial state fusion methods is validated and compared in simulations for various communication topologies with constant and Rankine wind models.

Keywords: wind estimation, multi-agent system, state fusion, EKF, covariance intersection

1. INTRODUCTION

Wind patterns and flow structures in the atmospheric boundary layer (ABL) are diverse and complex Wetz et al. (2021); González-Rocha et al. (2019). Wind field information can enhance safety, efficiency and robustness of small unmanned aircraft vehicles (sUAV) operations in low-altitude airspace. In addition, sUAV has become an alternative option for meteorology and environmental study. Since sUAV is low-cost, flexible and easy to operate, using sUAV as a tool to estimate wind field has become popular in recent years Chen et al. (2022); Chen and Bai (2022); McConville et al. (2022); Hattenberger et al. (2022); Meier et al. (2022). However, most of the research focuses on wind estimation using a single UAV instead of multiple UAVs.

Multi-UAV system can be used for monitoring Xing et al. (2019), target-tracking Xu et al. (2022), and search and rescue mission Alotaibi et al. (2019). Even though the research on wind estimation using multi-UAV is limited, using multi-agent systems for spatial field estimation is popular. Existing approaches includes distributed filtering approaches, Voronoi cell based approaches, machine learning approaches, among others. Motivated by the aforementioned applications, we focus on applying a multi-UAV system to wind field estimation. The advantages of using UAV swarm to measure the wind field compared to a single UAV include: 1) multiple and flexible wind information in space can be sampled or estimated synchronously, 2) UAV swarm can collect more data and provide higher spatial-temporal resolution for wind field, 3) real-time fusion of each quadcopter's data can increase convergence speed and reduce estimation error.

In Bai (2018), a stable nonlinear observer to estimate a spatial vector is designed with vehicles modeled as unicycles. Chao and Chen (2010) model the wind by a series of partial differential equations and use groups of fixed-wing UAVs in the simulation with a certain formation to measure the horizontal wind profiling simultaneously. Xing et al. (2019) estimate the wind based on wind triangle, and a recursive least-squares estimator is designed to estimate the wind speed with online measurements collected by a fleet of UAVs located in a circle trajectory. Wetz et al. (2021) describe a wind estimation method based on aerodynamic drag and quadcopter dynamics. Then a fleet of quadcopters is deployed to hover in different locations in a wind field. The main advantage of this approach is that multiple measurement points can be sampled synchronously. Overall, existing multi-UAV wind estimation approaches deploy the UAVs as a group of wind sensors located in various locations without considering real-time information fusion between the UAVs.

As capabilities for airborne communication and networking keep improving, it is expected that UAVs can achieve real-time or in-time airborne communication to share information. Real-time fusion of the wind estimate and its covariance from each UAV can result in accurate wind estimation that may not be attainable by a single UAV functioning in isolation, thereby improving performance of relevant downstream missions. The primary objective of fusing the estimated wind information from multiple UAVs is to obtain a more accurate and comprehensive assessment of the wind. State fusion architectures can be broadly classified into centralized fusion architecture and distributed fusion architecture. While centralized fusion can provide theoretically optimal solutions, it is not scalable to a large number of nodes. As the number of the nodes increases, processing all sensor measurements at one node becomes either ineffective or impractical due to communication overhead and reliability degradation Abu Bakr and Lee (2017). On the other hand, distributed fusion is more resilient to failures and requires less infrastructure and communication costs.

⋆ The work is supported by the National Science Foundation (NSF) under Grant No. 1925147.

10.1016/j.ifacol.2023.12.001

Because local estimates can be correlated, distributed fusion needs to take the correlations among the local estimates into consideration Abu Bakr and Lee (2017). Ignoring the cross-correlation can result in overconfident outcomes and even cause the fusion algorithm to fail. Consensus Battistelli et al. (2014) is a tool of averaging distributed information but it requires multiple communication iterations at each timestamp. To be more efficient, covariance intersection (CI) Julier and Uhlmann (2007) can fuse information pairs under unknown correlation with one-hop communication. In multi-UAV wind estimation, each UAV maintains an estimator which contains the ownship states (UAV's own states such as position, velocity and attitude) and target states (wind vector or wind parameters). Fusing the wind estimates can be treated as a partial state decentralized data fusion (DDF) problem. The factorized weighted exponential product (WEP) in Ahmed et al. (2016); Ahmed (2014) is designed for performing partial state DDF.

The main contribution of this paper is as follows. 1) We design iterative nonlinear distributed wind fusion methods by integrating EKF, with sequential CI (SCI) and sequential WEP (SWEP). Such methods fuse wind estimates as well as covariance under unknown correlations. Since each agent's information is shared and fused, the wind field estimation of each quadcopter is expected to converge faster with better accuracy. 2) We verify and compare various multi-UAV wind field estimation methods under different wind fields and communication graphs. The simulation results show that EKF with fusion has less error and converges faster for wind field estimation when compared to that of EKF without fusion.

The rest of the paper is organized as follows. In Section 2, we introduce the single quadcopter dynamics in the presence of wind and extend it to model multi-quadcopter in a spatial wind field. In Section 3, we present the multi-UAV wind field estimation algorithms for EKF without fusion, EKF with SCI fusion, and EKF with SWEP fusion. Section 4 provides simulation results of the designed methods. Conclusions and future work are discussed in Section 5.

2. PROBLEM FORMULATION

2.1 Quadcopter dynamics in wind

The translational dynamics and attitude kinematics of a quadcopter subject to a wind disturbance in the north-east-down (NED) frame is given by

$$\begin{aligned} \dot{x} &= q * v_r * q^{-1} + v_w, v_w = F(x,d) \\ \dot{v}_r &= v_r \times \omega + q^{-1} * \boldsymbol{g} * q + \frac{1}{m}\boldsymbol{f}_c + \frac{1}{m} f_d \\ \dot{q} &= \frac{1}{2} q * \omega \\ \dot{d} &= 0 \end{aligned} \tag{1}$$

where $x \in \mathbb{R}^3$ is the inertial position, $v_r = q^{-1} * (v_g - v_w) * q \in \mathbb{R}^3$ is the relative velocity in the body frame, and $v_g \in \mathbb{R}^3$ and $v_w \in \mathbb{R}^3$ are the ground and wind velocity in the inertial frame respectively, d denotes the constant parameters in a spatial wind field $F(x,d)$, $q \in \mathbb{R}^4$ is the unit quaternion which represents quadcopter's orientation with respect to the inertial frame, and $*$ denotes the quaternion multiplication in which any vector in $\mathbb{R}^3$ is augmented to a quaternion with 0 being the scalar part, $\omega \in \mathbb{R}^3$ is the angular velocity in the body frame, $\boldsymbol{g} = [0,0,g]^T \in \mathbb{R}^3$ denotes the gravity acceleration vector in inertial frame, $\boldsymbol{f_c} = [0,0,-f_c]^T \in \mathbb{R}^3$ denotes the thrust vector in body frame where f_c is the amplitude of the thrust control input, and f_d denotes the drag force due to air resistance. We use a quadratic thrust model as shown below where ρ is the air density and D denotes the drag coefficient matrix:

$$f_d = -\frac{1}{2}\rho D |v_r| v_r, \;\; D = \begin{pmatrix} D_x & 0 & 0 \\ 0 & D_y & 0 \\ 0 & 0 & D_z \end{pmatrix}. \tag{2}$$

For thrust model, we use the nominal thrust model $f_c = k_\Omega \sum_{i=1}^4 \Omega_i^2$ where k_Ω is the thrust coefficient and Ω_i is the angular speed of the each rotor.

We define the quadcopter's ownship state vector as $s = [x^T \;\; v_r^T \;\; q^T]^T$ and the full state vector as $X = [s^T \;\; d^T]^T$. We also define the measured angular velocity from the gyroscope and the thrust f_c as an input vector $U = [f_c \;\; \omega^T]^T$. We assume that the quadcopter is equipped with a GPS, a 3-axis accelerometer and gyroscope, and a magnetometer. We assume that biases of the sensors are calibrated. The measured outputs $y = (y_x^T, y_a^T, y_b^T)^T$ are

$$y = h(X,U) = \begin{pmatrix} x \\ a \\ q^{-1} * B * q \end{pmatrix} \tag{3}$$

where $B \in \mathbb{R}^3$ denotes the earth's magnetic field in the inertial frame and $a = \frac{1}{m}(\boldsymbol{f_c} + f_d) \in \mathbb{R}^3$ is the specific acceleration vector in the body frame.

2.2 Multiple quadcopters in a wind field

Consider a network of N quadcopters hovering in a wind field v_w. The system dynamics for the quadcopter swarm is given by

$$\begin{aligned} \dot{x}_i &= q_i * v_{r,i} * q_i^{-1} + v_{w,i}, v_{w,i} = F(x_i,d) \\ \dot{v}_{r,i} &= v_{r,i} \times \omega_i + q_i^{-1} * \boldsymbol{g} * q_i + \frac{1}{m}\boldsymbol{f}_{c,i} + \frac{1}{m} f_{d,i} \\ \dot{q}_i &= \frac{1}{2} q_i * \omega_i \\ \dot{d} &= 0. \end{aligned} \tag{4}$$

where $v_{w,i}$ is the wind vector at quadcopter $i's$ location and the function $F(x_i,d)$ is a general representation of a spatial wind field parameterized by a constant parameter d.

We employ a directed graph $G = (V,E)$ to represent the communication topology between the quadcopters, where $V = \{1,...,N\}$ denotes the set of the quadcopters (agents) and $E \in V \times V$ denotes the set of communication links between the agents. We assume that each agent contains self loops, i.e.,$(i,i) \in E$. We define agent $i's$ neighboring set as $N_i = \{j | (j,i) \in E, j \in V\}$. The cardinality of N_i is n_i.

Since different quadcopters are deployed at different locations x_i, they experience different wind $v_{w,i}$ and thus their estimates of d may contain different information. The objective is to design fusion mechanisms among the quadcopters to combine their estimates of d and obtain a joint estimate of the wind field. We expect that the jointly estimated wind field is more accurate and converges faster.

3. MULTI-QUADCOPTER WIND ESTIMATION

In this section, we first introduce the design for an EKF wind estimator, which will be used by each quadcopter to estimate wind separately. Then two partial state DDF methods, SCI and SWEP, will be designed with the EKF.

3.1 EKF-WIO

The baseline of our multi-quadcopter wind estimation is an EKF without fusion of neighbors' information, which we call *EKF-WIO*. Such a method is similar to most of existing multi-UAV wind estimation methods since there is no information sharing among the quadcopters. The designed EKF is a continuous-discrete EKF Beard (2008) whose prediction step is propagated in a continuous way while the correction step is done in discrete time. To derive the EKF algorithm, we consider multiplicative process noise in the system dynamics and obtain

$$\begin{aligned}
\dot{x}_i &= q_i * v_{r,i} * q_i^{-1} + v_{w,i} + w_x \\
\dot{v}_{r,i} &= v_{r,i} \times (\omega_i + w_\omega) + q_i^{-1} * \boldsymbol{g} * q_i + \frac{1}{m}(\boldsymbol{f}_{c,i} + \boldsymbol{w_f}) + \frac{1}{m} f_{d,i} \\
\dot{q}_i &= \frac{1}{2} q_i * (\omega_i + w_\omega) \\
\dot{d} &= 0 + w_d,
\end{aligned} \tag{5}$$

where $\boldsymbol{w}_f = [0,0,w_f]^T$ and $w = [w_x^T, w_\omega^T, w_f, w_d^T]^T \in \mathbb{R}^{10}$ are process noises. The pseudo code for a single EKF is shown in algorithm 1.

Algorithm 1 EKF

```
Initialize X̂, P̂
for k ← 1 to K do
    Prediction: in between measurements (t ∈ [t_{k-1}, t_k])
    propagate X̂̇ = f(X̂, U) to obtain X̂_k^-
    A = ∂f/∂X, L = ∂f/∂w
    propagate P̂ = AP̂ + P̂A^T + LQL^T to obtain P̂_k^-
    Correction: at the k^th sensor measurement (t = t_k)
    H_k = ∂y/∂X
    K_k = P̂_k^- H_k (H_k P̂_k^- H^T + R)^{-1}
    X̂_k^+ = X̂_k^- + K_k (y_{m,k} - h(X̂_k^-, U_k))
    P̂_k^+ = (I - K_k H) P̂_k^-
end for
```

3.2 EKF-SCI

Before we employ covariance intersection to fuse estimates between quadcopter i and j, there are two extra steps to be done. First, we define $s_j = [x_j^T \; v_{r,j}^T \; q_j^T]^T$ as the local state vector of quadcopter j. Let quadcopter j marginalize out s_j from its joint Gaussian probability density function (pdf) to produce the marginal Gaussian pdf $p_j(d_j) \sim \mathcal{N}(\hat{d}_j, {}^d\hat{P}_j)$ for the wind estimates, where the marginal sufficient statistics are obtained by removing the rows and columns corresponding to s_j from the mean vector and covariance matrix of the Gaussian distribution over X_j. Second, let quadcopter j 'extend' the distribution $p_j(d_j)$ to include local states of platform i. However, since quadcopter j does not have any information about s_i, quadcopter j augments ${}^dP_j$ with infinity on the diagonal elements and zeros on off-diagonal elements, which yields platform j's pseudo-joint distribution $p_j(s_i, d_j) \sim \mathcal{N}(\hat{X}_j, {}^X\hat{P}_j)$ as

$$\hat{X}_j = \begin{bmatrix} s_i \\ d_j \end{bmatrix}, {}^X\hat{P}_j = \begin{bmatrix} \infty & 0 \\ 0 & {}^dP_j \end{bmatrix}. \tag{6}$$

We fuse it with $p_i(s_i, d_i) \sim \mathcal{N}(\hat{X}_i, {}^X\hat{P}_i)$ via covariance intersection, i.e.,

$${}^X\hat{P}_{f,i}^{-1} = \omega_i {}^X\hat{P}_i^{-1} + (1-\omega_i) \begin{bmatrix} \infty & 0 \\ 0 & {}^d\hat{P}_j \end{bmatrix}^{-1} \tag{7}$$

$$\hat{X}_{f,i} = {}^X\hat{P}_{f,i} \left(\omega_i \, {}^X\hat{P}_i^{-1} \hat{X}_i + (1-\omega_i) \begin{bmatrix} \infty & 0 \\ 0 & {}^d\hat{P}_j \end{bmatrix}^{-1} \begin{bmatrix} s_i \\ d_j \end{bmatrix} \right) \tag{8}$$

where $\omega_i \in [0,1]$ is a weight.

We choose ω_i to minimize the trace of the fused covariance matrix, i.e., $\min_{\omega_i} \; J = tr({}^X\hat{P}_{f,i})$. Finding the optimal ω_i is a one-dimensional optimization problem, which can be solved by a binary search method. For fusing more than two data sources, we make use of the sequential covariance intersection (SCI) as shown in Deng et al. (2012). By integrating the designed EKF wind estimator with SCI data fusion, we develop our EKF-SCI algorithm and the pseudo code is shown in Algorithm 2.

3.3 EKF-SWEP

In Ahmed (2014), a weighted exponential product (WEP) rule was proposed to fuse estimates when correlation is unknown, i.e.,

$$p_{f,i}(X) \propto p_i(X)^\omega p_j(X)^{1-\omega}, \omega \in [0,1]. \tag{9}$$

Applying the conditional factorized WEP to our wind estimation problem with multiple quadcopters leads to the following

$$\begin{aligned}
p_{f,i}(s_i, d) &= p_{f,i}(d) p_{f,i}(s_i|d) \\
&= p_i(d)^\omega \; p_j(d)^{1-\omega} \; p_i(s_i|d) \\
&= p_i(d)(p_i(d)^{\omega-1} p_j(d)^{1-\omega}) p_i(s_i|d) \\
&= p_i(d) \; p_i(s_i|d) \; (p_i(d)^{\omega-1} p_j(d)^{1-\omega}) \\
&= p_i(s_i, d) g_{i,j}(d; \omega)
\end{aligned} \tag{10}$$

where $g_{i,j} = p_i(d)^{\omega-1} p_j(d)^{1-\omega}$ is an unnormalized Gaussian function given by

$$\begin{aligned}
g_{ij} &\sim \mathcal{N}(\hat{d}_f, {}^d\hat{P}_f) \\
{}^d\hat{P}_f &= \left((\omega - 1) \, {}^d\hat{P}_i^{-1} + (1-\omega) \, {}^d\hat{P}_j^{-1} \right)^{-1} \\
\hat{d}_f &= {}^d\hat{P}_f \left((\omega - 1) \, {}^d\hat{P}_i^{-1} \, \hat{d}_i + (1-\omega) \, {}^d\hat{P}_j^{-1} \, \hat{d}_j \right).
\end{aligned} \tag{11}$$

The updated Gaussian joint pdf over d and s_i is given by

$$\begin{aligned}
p_{f,i}(s_i, d) &\sim \mathcal{N}(\hat{X}_{f,i}, {}^X\hat{P}_{f,i}) \\
{}^X\hat{P}_{f,i} &= \left({}^X\hat{P}_i^{-1} + \begin{bmatrix} 0 & 0 \\ 0 & {}^d\hat{P}_f^{-1} \end{bmatrix} \right)^{-1} \\
\hat{X}_{f,i} &= {}^X\hat{P}_{f,i} \left({}^X\hat{P}_i^{-1} \, \hat{X}_i + \begin{bmatrix} 0 \\ {}^d\hat{P}_f^{-1} \, \hat{d}_f \end{bmatrix} \right).
\end{aligned} \tag{12}$$

Therefore, we can derive a 2-step process to address this fusion problem: 1) perform SCI fusion on the marginal estimates for d from each platform according to (11); 2) perform a local update for s_i at quadcopter i conditioned on the newly SCI-updated estimate for d based on (12). Similarly, when it comes to fuse more than two data sources, we use the sequential WEP (SWEP). The optimal weight is also obtained by a binary search method to minimize the trace of the fused covariance matrix. The pseudo code is shown in Algorithm 3.

4. SIMULATION RESULTS

4.1 Simulation setup

Our simulator is developed based on the MATLAB simulator in Soria et al. (2020). We adapt the simulator to include

Algorithm 2 EKF-SCI

Initialize $\hat{X}, \hat{P}$ for each quadcopter
for $k \leftarrow 1$ to K **do**
  for $i \leftarrow 1$ to N **do**
    $(\hat{X}_i, {}^{X}\hat{P}_i) = EKF(\hat{X}_{i,k-1}, {}^{X}\hat{P}_{i,k-1})$
  end for
  for $i \leftarrow 1$ to N **do**
    for $j \leftarrow 1$ to n_i **do**
      marginalize $p_j(s_j, d_j)$ **to get** $p_j(d_j) \sim \mathcal{N}(\hat{d}_j, {}^{d}\hat{P}_j)$
      extend $p_j(d_j) \sim \mathcal{N}(\hat{d}_j, {}^{d}\hat{P}_j)$ as
      $p_j(s_i, d_j) \sim \mathcal{N}(\hat{X}_j, {}^{X}\hat{P}_j)$
      Covariance Intersection **:**
      ${}^{X}\hat{P}_{f,i}^{-1} = \omega_i \, {}^{X}\hat{P}_i^{-1} + (1-\omega_i) \, {}^{X}\hat{P}_j^{-1}$
      $\hat{X}_{f,i} = {}^{X}\hat{P}_{f,i}(\omega_i \, {}^{X}\hat{P}_i^{-1}\hat{X}_i + (1-\omega_i) \, {}^{X}\hat{P}_j^{-1}\hat{X}_j)$
    end for
  end for
end for

Algorithm 3 EKF-SWEP

Initialize $\hat{X}, \hat{P}$ for each quadcopter
for $k \leftarrow 1$ to K **do**
  for $i \leftarrow 1$ to N **do**
    $(\hat{X}_i, {}^{X}\hat{P}_i) = EKF(\hat{X}_{i,k-1}, {}^{X}\hat{P}_{i,k-1})$
  end for
  for $i \leftarrow 1$ to N **do**
    marginalize i **and all its neighbors to obtain** $p_i(d)$ **and** $p_j(d)$
    for $j \leftarrow 1$ to n_i **do**
      Fuse Wind **:**
      ${}^{d}\hat{P}_{f,i} = \left((\omega_i - 1) {}^{d}\hat{P}_i^{-1} + (1-\omega_i) {}^{d}\hat{P}_j^{-1}\right)^{-1}$
      $\hat{d}_{f,i} = {}^{d}\hat{P}_{f,i}\left((\omega_i - 1) \, {}^{d}\hat{P}_i^{-1}\hat{d}_i + (1-\omega_i) \, {}^{d}\hat{P}_j^{-1}\hat{d}_j\right)$
    end for
    Fuse Full State **:**
    ${}^{X}\hat{P}_{f,i} = \left({}^{X}\hat{P}_i^{-1} + \begin{bmatrix} 0 & 0 \\ 0 & {}^{d}P_{f,i}^{-1} \end{bmatrix}\right)^{-1}$
    $\hat{X}_{f,i} = {}^{X}\hat{P}_{f,i}\left({}^{X}\hat{P}_i^{-1}\hat{X}_i + \begin{bmatrix} 0 \\ {}^{d}\hat{P}_{f,i}^{-1}\hat{d}_{f,i} \end{bmatrix}\right)$
  end for
end for

quadcopter system dynamics, motor and rotor models, sensor models, estimators, and position and attitude controllers. We conduct Monte Carlo (MC) simulations of 50 runs and each simulation lasts for 100 seconds. We choose a total number of 4 quadcopters as an example for demonstration.

We consider three different communication scenarios, including a fully connected graph, a ring graph, and a gossip protocol. The adjacency matrices for the fully connected graph and the ring graph are given by

$$A_{d,\text{fully}} = \begin{bmatrix} 0 & 1 & 1 & 1 \\ 1 & 0 & 1 & 1 \\ 1 & 1 & 0 & 1 \\ 1 & 1 & 1 & 0 \end{bmatrix}, A_{d,\text{ring}} = \begin{bmatrix} 0 & 1 & 0 & 1 \\ 1 & 0 & 1 & 0 \\ 0 & 1 & 0 & 1 \\ 1 & 0 & 1 & 0 \end{bmatrix}, \tag{13}$$

respectively. For the gossip-based protocol, two quadcopters are randomly selected at each time instant to communicate.

We let each quadcopter fly from the origin to $[100\ 100\ -20]^T, [100\ -100\ -40]^T, [-100\ -100\ -60]^T, [-100\ 100\ -100]^T$ in the NED frame, respectively and then hover at its location. The following parameters are used in all the simulations:

$$\mu_{0,i} = [0,0,0,0,0,0,1,0,0,0,0,0,0]^T$$
$$P_{0,i} = diag(1^2, 1^2, 1^2, 1^2, 1^2, 1^2, 1^2, 1^2, 1^2, 1^2, 1^2, 1^2, 1^2)$$
$$\hat{X}_{0,i} \sim \mathcal{N}(\mu_{0,i}, P_{0,i})$$

where $\hat{X}_{0,i}$ and $P_{0,i}$ represents the initial states and covariance matrix used in each quadcopter's EKF. The process and measurement noise covariance matrices for the EKF are

$$Q = [diag(0.1, 0.1, 0.1, 0.0023, 0.0023, 0.0023, 0, 0.001, 0.001, 0.001)]^2$$
$$R = [diag(0.1, 0.1, 0.1, 0.025, 0.025, 0.025, 0.001, 0.001, 0.001)]^2.$$

4.2 Comparison results

We first compare the EKF-WIO, EKF-SCI and EKF-SWEP wind estimation performance under three various communication topology when the wind field is spatially uniform. Then We compare the EKF-WIO, EKF-SCI and EKF-SWEP when the wind field is spatially-varying using a Rankine model.

Constant wind We consider a constant wind field, i.e.,

$$v_w = F(x, d) = [d_1 \ d_2 \ d_3]^T, \tag{14}$$

and focus on the horizontal wind estimation where $d_1 = 1\ m/s$, $d_2 = 2\ m/s$, and $d_3 = 0\ m/s$. Fig. 1(a) shows wind estimation performance with EKF-WIO from one simulation in the MC runs. Fig. 1(b) and Fig. 1(c) show wind estimation performance based on EKF-SCI and EKF-SWEP. Both algorithms produce improved performance compared to EKF method without fusion. The transient error has been reduced and the estimates from all the UAVs show a consensus trend.

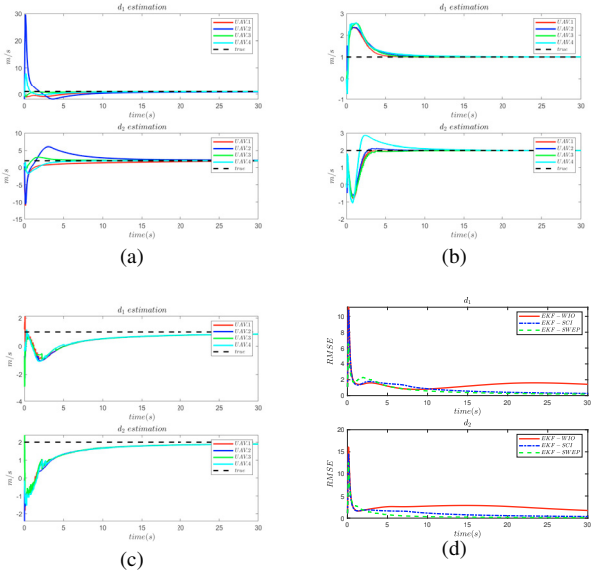

Fig. 1. Single run and MC simulation examples (first 30 seconds) under fully connected graph. (a) EKF-WIO constant wind estimation (b) EKF-SCI constant wind estimation (c) EKF-SWEP constant wind estimation (d) Comparison of $RMSE_k$ of EKF-WIO, EKF-SCI and EKF-SWEP under constant wind

For MC simulation results, wind estimation performance of various methods is evaluated by root mean square error (RMSE). For example, the RMSE of wind d (d_1 or d_2) for quadcopter i at each time instant k is as $RMSE_{k,i} = \sqrt{\frac{\sum_{m=1}^{N_m}(d_{k,i} - \hat{d}_{k,i})^2}{N_m}}$ where

Table 1. Constant wind estimation RMSE of EKF-WIO, EKF-SCI and EKF-SWEP under fully connected graph (FG), ring graph (RG) and gossip protocol (GP)

Method	d_1/d_2	$RMSE_{trans}$	$RMSE_{steady}$	$RMSE_{total}$
EKF-WIO	d_1	1.4545	0.4036	0.9213
EKF-WIO	d_2	2.7238	0.4539	1.3355
EKF-SWEP (FG)	d_1	1.3288	0.0467	0.2687
EKF-SWEP (FG)	d_2	1.3285	0.0258	0.2031
EKF-SCI (FG)	d_1	1.3537	0.0681	0.3489
EKF-SCI (FG)	d_2	1.9447	0.0879	0.4342
EKF-SWEP (RG)	d_1	1.2985	0.0388	0.2345
EKF-SWEP (RG)	d_2	1.3738	0.0320	0.2248
EKF-SCI (RG)	d_1	1.3676	0.0689	0.3525
EKF-SCI (RG)	d_2	1.9450	0.0879	0.4344
EKF-SWEP (GP)	d_1	1.3237	0.0406	0.2420
EKF-SWEP (GP)	d_2	1.3623	0.0290	0.2159
EKF-SCI (GP)	d_1	1.3698	0.0692	0.3537
EKF-SCI (GP)	d_2	1.9440	0.0880	0.4344

$N_m = 50$ is the total runs of MC simulations. Since RMSE of single quadcopter does not represent the overall swarm wind estimation performance, we introduce mean RMSE of all quadcopters at the kth time instant $RMSE_k = \frac{\sum_{i=1}^{N} RMSE_{k,i}}{N}$ where $N = 4$ is total number of the quadcopter swarm. We further compute the average of $RMSE_k$ over different time periods, including the first 10 seconds, the last 10 seconds, and the entire 100 seconds, to show transient, steady-state, and overall performance of various methods, respectively. They are represented by $RMSE_{trans}$, $RMSE_{steady}$, and $RMSE_{total}$ as shown below

$$RMSE_{trans} = \frac{\sum_{k=1}^{10 f_e} RMSE_k}{10 f_e} \tag{15}$$

$$RMSE_{steady} = \frac{\sum_{k=(K-10) f_e}^{K f_e} RMSE_k}{10 f_e} \tag{16}$$

$$RMSE_{total} = \frac{\sum_{k=1}^{K f_e} RMSE_k}{K f_e}. \tag{17}$$

where $K = 100$ is total time of one-run MC simulation and $f_e = 100$ is the frequency of the EKF.

Table 1 compares the constant wind estimation performance of EKF-WIO, EKF-SCI and EKF-SWEP under the fully connected graph, the ring graph and the gossip protocol, respectively. Fig. 1(d) shows the $RMSE_k$ of three different methods under the fully connected graph. We observe that 1) the EKF with either fusion algorithm (EKF-SCI or EKF-SWEP) reduces the transient, steady and total RMSE and accelerates convergence speed when compared to EKF-WIO. 2) EKF-SWEP shows slightly better overall performance compared to EKF-SCI for constant wind. 3) The fusion algorithms appear robust to different communication topologies.

Rankine Wind We also use a Rankine wind model to evaluate the performance of the fusion algorithms. The spatial model of the wind is given by $v_w = G(x)d$ where $G(x) \in \mathbb{R}^{n\times n}$ is a known basis function matrix, and the $d \in \mathbb{R}^n$ is the unknown parameter vector. The Rankine vortex model is a simple two-equation parametric description of a swirling flow and it is usually used for tornado and cyclone modeling. We use the following model from Bai (2018)

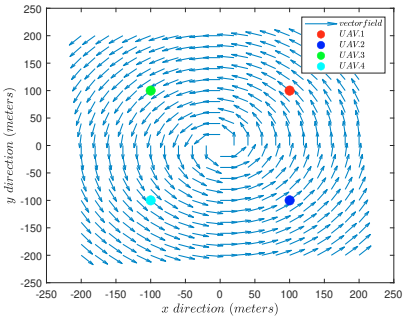

Fig. 2. Multiple UAVs hover in the Rankine wind field

$$v_w = F(x,d) = \begin{bmatrix} G_1(x)d_1 \\ G_2(x)d_2 \\ d_3 \end{bmatrix} \tag{18}$$

$$G_1(x) = -\frac{x_2}{2\pi\sqrt{x_1^2+x_2^2}}, G_2(x) = \frac{x_1}{2\pi\sqrt{x_1^2+x_2^2}}. \tag{19}$$

The Rankine wind model is only applicable to horizontal wind. The vertical wind is modeled as a constant wind. We set $d_1 = 10$ and $d_2 = 20$, and $d_3 = 0$ m/s. Figure 2 shows 4 quadcopters hovering in the spatial-varying Rankine wind field. We assume that the center point of the wind field is available.

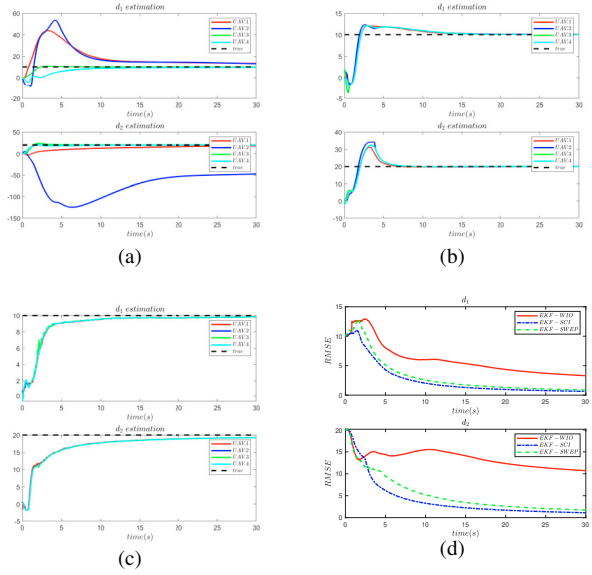

Fig. 3. Single run and MC simulation examples (first 30 seconds) under fully connected graph. (a) EKF-WIO Rankine wind estimation (b) EKF-SCI Rankine wind estimation (c) EKF-SWEP Rankine wind estimation (d) Comparison of $RMSE_k$ of EKF-WIO, EKF-SCI and EKF-SWEP under Rankine wind

Figure 3(a) shows wind parameters estimation of EKF-WIO from single run of MC 50 tests. The estimation performance is worse compared to that of constant wind. The estimates of wind parameters of some quadcopters converge to wrong values, suggesting an observability issue when each quadcopter is operated independently. Fig. 3(b) and Fig. 3(c) show the estimation of wind parameters of EKF-SCI and EKF-SWEP from one run of the MC tests. We observe that the estimation of the wind parameters achieves consensus, converges faster and produces less error since fusion of the wind estimates results in better observability.

Table 2. Rankine wind estimation RMSE of EKF-WIO, EKF-SCI and EKF-SWEP under fully connected graph (FG), ring graph (RG) and gossip protocol (GP)

Method	d_1/d_2	$RMSE_{trans}$	$RMSE_{steady}$	$RMSE_{total}$
EKF-WIO	d_1	8.8900	1.9653	3.4603
EKF-WIO	d_2	14.9661	8.4296	10.3817
EKF-SWEP (FG)	d_1	6.3985	0.2723	1.2364
EKF-SWEP (FG)	d_2	10.0391	0.5442	2.1967
EKF-SCI (FG)	d_1	5.4799	0.2249	1.0048
EKF-SCI (FG)	d_2	8.5168	0.3146	1.5954
EKF-SWEP (RG)	d_1	6.7589	0.2836	1.3114
EKF-SWEP (RG)	d_2	10.3030	0.5485	2.2303
EKF-SCI (RG)	d_1	6.0164	0.2643	1.1449
EKF-SCI (RG)	d_2	11.0714	0.5625	2.4019
EKF-SWEP (GP)	d_1	6.6208	0.2993	1.3158
EKF-SWEP (GP)	d_2	10.1753	0.5455	2.2116
EKF-SCI (GP)	d_1	6.6103	0.2921	1.2788
EKF-SCI (GP)	d_2	10.1586	0.4314	1.9954

Table 2 compares the Rankine wind estimation performance of EKF-WIO, EKF-SCI and EKF-SWEP under the fully connected graph, the ring graph and the gossip protocol, respectively. We observe that: 1) EKF without fusion shows much larger RMSE for various communication graphs compared to EKF with fusion. 2) EKF-SCI and EKF-SWEP perform similarly. Fig. 3(d) shows the $RMSE_k$ of three methods under the fully connected graph.

Based on the simulation results, both EKF fusion algorithms achieve improved performance for multi-UAV wind field estimation, when compared to EKF without fusion. Considering the similar estimation performance and the ease of implementation, EKF-SCI would be a better option.

5. CONCLUSION

We formulate a spatial wind field estimation problem using multiple quadcopters. We develop EKFs with the SCI and SWEP fusion methods, which fuse wind state estimates as well as their covariance. We conduct MC simulations and evaluate the wind estimation performance for EKF-WIO, EKF-SCI and EKF-SWEP under various communication topologies. The MC simulations show that wind field estimation using EKF with fusion methods has less error and converges faster when compared to EKF without fusion. Future work includes designing invariant EKF for spatial-temporal wind estimation with multiple quadcopters.

REFERENCES

Abu Bakr, M. and Lee, S. (2017). Distributed multisensor data fusion under unknown correlation and data inconsistency. *Sensors*, 17(11), 2472.

Ahmed, N. (2014). Conditionally factorized ddf for general distributed bayesian estimation. In *2014 International Conference on Multisensor Fusion and Information Integration for Intelligent Systems (MFI)*, 1–7. IEEE.

Ahmed, N.R., Whitacre, W.W., Moon, S., and Frew, E.W. (2016). Factorized covariance intersection for scalable partial state decentralized data fusion. In *2016 19th International Conference on Information Fusion (FUSION)*, 1049–1056. IEEE.

Alotaibi, E.T., Alqefari, S.S., and Koubaa, A. (2019). Lsar: Multi-UAV collaboration for search and rescue missions. *IEEE Access*, 7, 55817–55832.

Bai, H. (2018). Motion-dependent estimation of a spatial vector field with multiple vehicles. In *2018 IEEE conference on decision and control (CDC)*, 1379–1384. IEEE.

Battistelli, G., Chisci, L., Mugnai, G., Farina, A., and Graziano, A. (2014). Consensus-based linear and nonlinear filtering. *IEEE Transactions on Automatic Control*, 60(5), 1410–1415.

Beard, R.W. (2008). Quadrotor dynamics and control. *Brigham Young University*, 19(3), 46–56.

Chao, H. and Chen, Y. (2010). Surface wind profile measurement using multiple small unmanned aerial vehicles. In *Proceedings of the 2010 American Control Conference*, 4133–4138. IEEE.

Chen, H. and Bai, H. (2022). Incorporating thrust models for quadcopter wind estimation. *IFAC-PapersOnLine*, 55(37), 19–24.

Chen, H., Bai, H., and Taylor, C.N. (2022). Invariant-EKF design for quadcopter wind estimation. In *2022 American Control Conference (ACC)*, 1236–1241. IEEE.

Deng, Z., Zhang, P., Qi, W., Liu, J., and Gao, Y. (2012). Sequential covariance intersection fusion kalman filter. *Information Sciences*, 189, 293–309.

González-Rocha, J., Woolsey, C.A., Sultan, C., and De Wekker, S.F. (2019). Sensing wind from quadrotor motion. *Journal of Guidance, Control, and Dynamics*, 42(4), 836–852.

Hattenberger, G., Bronz, M., and Condomines, J.P. (2022). Estimating wind using a quadrotor. *International Journal of Micro Air Vehicles*, 14, 17568293211070824.

Julier, S.J. and Uhlmann, J.K. (2007). Using covariance intersection for slam. *Robotics and Autonomous Systems*, 55(1), 3–20.

McConville, A., Richardson, T.S., and Moradi, P. (2022). Comparison of multirotor wind estimation techniques through conventional on-board sensors. In *AIAA SCITECH 2022 Forum*, 0411.

Meier, K., Hann, R., Skaloud, J., and Garreau, A. (2022). Wind estimation with multirotor uavs. *Atmosphere*, 13(4), 551.

Soria, E., Schiano, F., and Floreano, D. (2020). Swarmlab: A matlab drone swarm simulator. In *2020 IEEE/RSJ International Conference on Intelligent Robots and Systems (IROS)*, 8005–8011. IEEE.

Wetz, T., Wildmann, N., and Beyrich, F. (2021). Distributed wind measurements with multiple quadrotor unmanned aerial vehicles in the atmospheric boundary layer. *Atmospheric Measurement Techniques*, 14(5), 3795–3814.

Xing, Z., Zhang, Y., Su, C., and Qu, Y. (2019). Measuring the horizontal wind for forest fire monitoring using multiple uavs. In *2019 Chinese Control Conference (CCC)*, 4945–4950. IEEE.

Xu, J., Zhu, P., and Ren, W. (2022). Distributed invariant extended kalman filter for 3-d dynamic state estimation using lie groups. In *2022 American Control Conference (ACC)*, 2367–2372. IEEE.